Flexible Tri-Axis Tactile Sensor Using Spiral Inductor and Magnetorheological Elastomer

Takumi Kawasetsu, *Student Member, IEEE*, Takato Horii, *Member, IEEE*, Hisashi Ishihara, and Minoru Asada, *Fellow, IEEE*

***Abstract*— This paper describes a flexible and soft tactile sensor that measures the tri-axis force based on inductance measurement. The proposed sensor has four spiral inductors printed on a flexible circuit board and a mounted cylindrical elastomer (silicon rubber). A disk-shaped magnetorheological elastomer (ferromagnetic marker) is embedded in the cylindrical elastomer and its 3-D displacement is estimated by monitoring the inductance changes of the four inductors. In this paper, we investigated the relationship between the applied tri-axis force and inductance changes. Our results can be summarized as follows: 1) the inductance changes of the four inductors were monotonic and linear against the applied normal and shear force; 2) the applied tri-axis force could be estimated well with linear functions of the sum and difference of the measured inductances; and 3) the estimation error of the tri-axis force increased when a larger force was applied and/or faster contact speeds were used.**

***Index Terms*— Force and tactile sensing, tactile sensor, flexible sensor, magnetorheological elastomer, inductance measurement.**

I. Introduction

FLEXIBLE and soft tactile sensors play important roles in robotic systems interacting with unknown objects. A number of studies have proposed various types of tactile sensors (see reviews [1]–[3]) using elastic materials as their surface coverings. This is because flexible and soft sensor surfaces can fit the complex surfaces of objects safely both for the objects and the robot itself. In contrast, sensors containing soft materials suffer from several technical issues related to deteriorations in the fundamental properties of tactile sensors such as durability, sensitivity, and mechanical simplicity.

As one solution for these issues, we previously proposed and developed a flexible tactile sensor in which a sheet-shaped magnetorheological elastomer (MRE), which is a ferromagnetic silicon rubber, is laminated on a sheet-shaped silicon rubber covering a flexible circuit board with a spiral inductor [4]. Because the MRE contains iron particles with a high magnetic permeability, the distance between the MRE and inductor determines its inductance. Thus, the inductance increases/decreases in accordance with the descent/ascent of the MRE around the inductor, respectively. In the previous study, we demonstrated that the sensor could measure applied normal forces by monitoring the inductance of the inductor. The advantages of this sensor can be summarized as follows: 1) high durability–it has a durable structure against shocks and heavy loads because the flexible and soft surface where the contact force is applied contains no fragile electric transducers or wirings; 2) high sensitivity–it is sensitive to small forces because it directly captures surface deformations of the outermost soft MRE layer; 3) simple structure–its structure is simple and damaged surfaces are therefore easy to replace because the surface elastomer sheets are placed on the circuit board without any wire connections.

One of the biggest remaining issues is that the sensor cannot measure the tri-axis force, because of its structure. In this study, we improve the tactile sensor so that it can measure the tri-axis force without deteriorating the above advantages of the sensor. As shown in Fig. 1, the proposed tri-axis tactile sensor consists of four inductors, a disk-shaped MRE (hereafter called ferromagnetic marker or marker), and a cylindrical elastomer made of a silicon rubber. In this structure, applied normal and shear forces cause a vertical and horizontal displacement in the ferromagnetic marker, respectively.

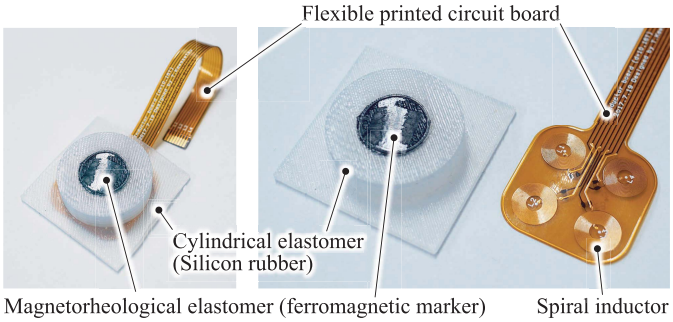

Fig. 1. Appearance of the proposed tri-axis tactile sensor. The sensor consists of four spiral inductors printed on a flexible printed circuit board (FPCB) and a disk-shaped magnetorheological elastomer (MRE; ferromagnetic marker) embedded in a cylindrical elastomer made of a silicon rubber. The inductances of the inductors are determined by the positional relationship between the ferromagnetic marker and each inductor because the marker contains iron particles with a high magnetic permeability. Therefore, the sensor can estimate applied tri-axis forces by monitoring the inductance changes caused by three-dimensional (3D) displacements of the marker.

Manuscript received April 17, 2018; revised May 30, 2018; accepted May 31, 2018. Date of publication June 5, 2018; date of current version June 26, 2018. This work was supported in part by JSPS KAKENHI under Grant JP17J01443, in part by the Tenure Track Program at the Frontier Research Base for Global Young Researchers, in part by the Center of Innovation Program from MEXT and JST, and in part by PRESTO, JST under Grant JPMJPR1652. The associate editor coordinating the review of this paper and approving it for publication was Prof. Ravinder S. Dahiya. *(Corresponding author: Takumi Kawasetsu.)*

T. Kawasetsu, H. Ishihara, and M. Asada are with the Department of Adaptive Machine Systems, Graduate School of Engineering, Osaka University, Suita 565-0871, Japan (e-mail: takumi.kawasetsu@ams.eng.osaka-u.ac.jp).

T. Horii is with the Department of Mechanical Engineering and Intelligent Systems, Graduate School of Informatics and Engineering, The University of Electro-Communications, Chofu 182-8585, Japan.

Digital Object Identifier 10.1109/JSEN.2018.2844194

As a result, the inductances of the four inductors indicate the three-dimensional (3D) position of the ferromagnetic marker. It is expected that: 1) the summation value of all inductances indicates the magnitude of an applied normal force because the vertical distances between the marker and every inductor decrease simultaneously; 2) the difference of the four inductance values indicates the direction and magnitude of an applied shear force because the horizontal distances between the marker and every inductor decreases or increases depending on the positions of the inductors. In contrast, the ferromagnetic marker itself is deformed by the contact force because the marker is made with a highly flexible and soft silicon rubber. Such deformation of the ferromagnetic marker might affect the expected inductance changes mentioned above. In addition, the non-linear rubber elasticity might cause a nonlinear change in inductance. Therefore, the relationship between the applied tri-axis force and inductance should be investigated to enable the measurement of the tri-axis force.

In order to investigate this relationship, we measured the sensor responses by using the developed sensor. The results can be summarized as follows: 1) the inductance changes of the four inductors were monotonic and linear against an applied normal and shear force; 2) the applied tri-axis force could be estimated well with linear functions of the sum and difference of the measured inductances; 3) the estimation error of the tri-axis force increased against a larger force or faster contact speeds.

The remainder of this article is organized as follows. Section II reviews and discusses the issues of conventional soft tri-axis tactile sensors. Section III introduces the developed tri-axis tactile sensor and its sensing mechanism. Section IV describes the experimental methods and results, which are then discussed in Sec. V. Finally, the conclusions and future research are presented in Section VI.

II. State-of-the-Art Tactile Sensors

This section summarizes conventional, tri-axis tactile sensors covered with thick and soft coverings and their issues to be addressed. Several review papers have also introduced state-of-the-art tactile sensors [1]–[3]. Here, we categorize existing soft tri-axis tactile sensors into four types according to their sensing mechanisms and structures, as shown in Fig. 2.

Figure 2 (a) shows an illustration of the first sensor type, which is a tri-axis tactile sensor using micro-cantilevers embedded in an elastic material as a strain transducer (Fig. 2(a)) [5]–[10]. Applied tri-axis forces deform the elastic material and the cantilevers inside the elastic material. The cantilevers mount in several orientations in order to detect the 3D deformation of the elastic material. In this structure, the tri-axis force can be estimated based on a combination of outputs from the cantilevers. One of the issues of this kind of sensor is that the transducers and their electrical wiring inside the elastic material deteriorate its durability, i.e., a large shock to the sensor may damage these elements.

Several papers have proposed magnetic tri-axis tactile sensors [11]–[16] in which a surface elastic material containing a permanent magnet is placed on a magnetic transducer

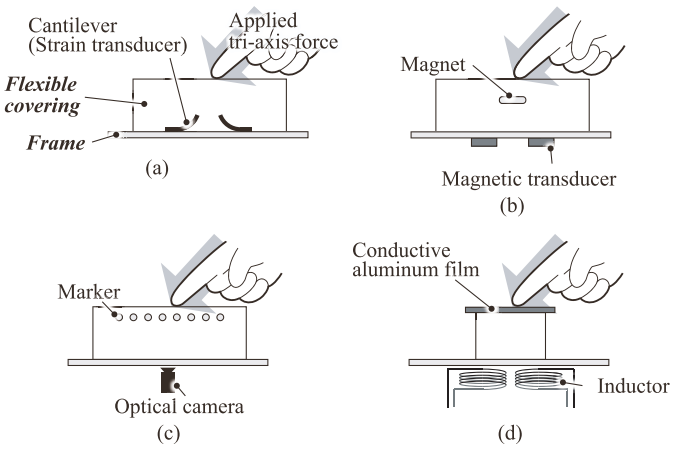

Fig. 2. Conventional flexible tri-axis tactile sensor covered with thick and soft coverings: (a) cantilevers, which function as a strain transducer, embedded in the flexible covering and directly detecting the tri-axis force applied to the covering; (b) magnetic transducers detecting the 3D displacement of a magnet embedded in the flexible covering; (c) optical camera capturing the 3D displacements of optical markers embedded in the flexible covering; and (d) inductors detecting the displacement of a non-stretchable conductive aluminum film based on the eddy-current effect.

(Fig. 2(b)). The sensor can measure the tri-axis force by monitoring the magnetic field change caused by the 3D displacement of the magnet. One of the advantages of this sensor is its high durability because the elastic material where contact force is applied contains no fragile electric transducers or wirings. In contrast, the solid magnets inside the soft surface deteriorates the softness of the surface.

Optical tri-axis tactile sensors [17]–[22] can also feasibly realize high durability because their elastic coverings also contain no transducers or wiring. They measure applied contact forces by monitoring the 3D displacement of color markers embedded in the elastic material based on the visual information from a camera (Fig. 2(c)). The advantage of optical tactile sensors is that the sensor can obtain force distribution information on a wide sensor surface with a high spatial resolution. The drawback is that the optical system in the sensor leads to a difficulty of miniaturization because the system requires an optical lens.

Recently, a tri-axis tactile sensor based on inductance measurements was proposed [23] (Fig. 2(d)). This sensor had a similar configuration to our proposed sensor; however, their sensor employed a different sensing mechanism, namely, the eddy-current effect, and their sensor thus used a conductive aluminum film instead of the ferromagnetic marker used in our sensor. Although the sensor can estimate the applied tri-axis force by monitoring the four inductances changes caused by the 3D displacement of the film, the nonstretchable film deteriorates the softness and the stretchability of its top coverings.

In conclusion, conventional flexible tri-axis tactile sensors with thick elastic coverings suffer from technical issues such as fracturing of the sensing elements by a large contact force, implementation of a solid into the elastic cover, difficulty in miniaturization, deterioration of softness, and stretchability of its cover. The sensor we proposed can address these issues.

III. Proposed Tri-Axis Tactile Sensor

This section provides details of the developed sensor and its sensing mechanism.

A. Developed Sensor

We developed a four-inductor array to measure displacements of the ferromagnetic marker. As shown in Fig. 3(a), each inductor is printed on a flexible printed circuit board (FPCB) as a thin two-layer spiral inductor. In this study, we employed an FPCB manufacturing service (P-ban.com Corp., Japan). The FPCB is 30-mm wide, 30-mm long (except for the connecter part), and 12.5-μm thick. Each inductor has a diameter of 10 mm, and the number of turns is set to 16 in each layer. The trace width and spacing between the traces are both 100 μm. The thickness of the trace is set to 35 μm. In this study, we employed an inductance-to-digital converter that measures the inductances by detecting the resonant frequency on an LC parallel resonance circuit. Hence, a ceramic capacitor with a capacitance of 330 pF was connected in parallel with each inductor.

The design parameters of an inductor, such as the width and thickness of a trace, and the spacing between the traces, were determined to achieve a high Q factor in the LC parallel resonance circuit (please refer to [24] for more information). The trace width and spacing between traces should be narrow because the number of turns can be increased to achieve a high sensitivity. Therefore, we determined the width and spacing as 100 μm, which is the minimum value acceptable for the manufacturing service. In contrast, the thickness of the traces should be thick as much as possible because the parasitic resistance of the inductor should be reduced to achieve a higher Q factor. Therefore, we determined the thickness as 35 μm, which is the maximum value acceptable for the manufacturing service. As a reference, the Q factor in this study was 28.3 at a resonance frequency of 3.22 MHz, which was calculated by an inductor design tool [24].

Four inductors are arranged at equal intervals of 15 mm in the x- and y-directions, as illustrated in Fig. 3(b). Figure 3(c) shows an illustration of the sensor configuration for the experiments in this study. A plastic holder supports both the cylindrical elastomer containing the ferromagnetic marker and the FPCB containing the inductors. The bottom surface of the marker is raised by 8 mm from the FPCB top surface. The diameter and thickness of the ferromagnetic marker are set to 15 and 3 mm, respectively, while the diameter and thickness of the cylindrical elastomer are 30 and 10 mm, respectively. The ferromagnetic marker and cylindrical elastomer are composed of a platinum-cured silicone rubber (Ecoflex 00-30, Smooth-On, Inc., USA). To construct the ferromagnetic marker, iron particles with a diameter of 50 μm were mixed with the platinum-cured silicon rubber at a volume ratio of 40% before curing, and was poured into a disk-shaped female mold until cured (Fig. 4 (a)). Subsequently, the ferromagnetic marker was placed at the bottom of another female mold, and the platinum-cured silicon rubber was poured into the mold until cured (Fig. 4 (b)).

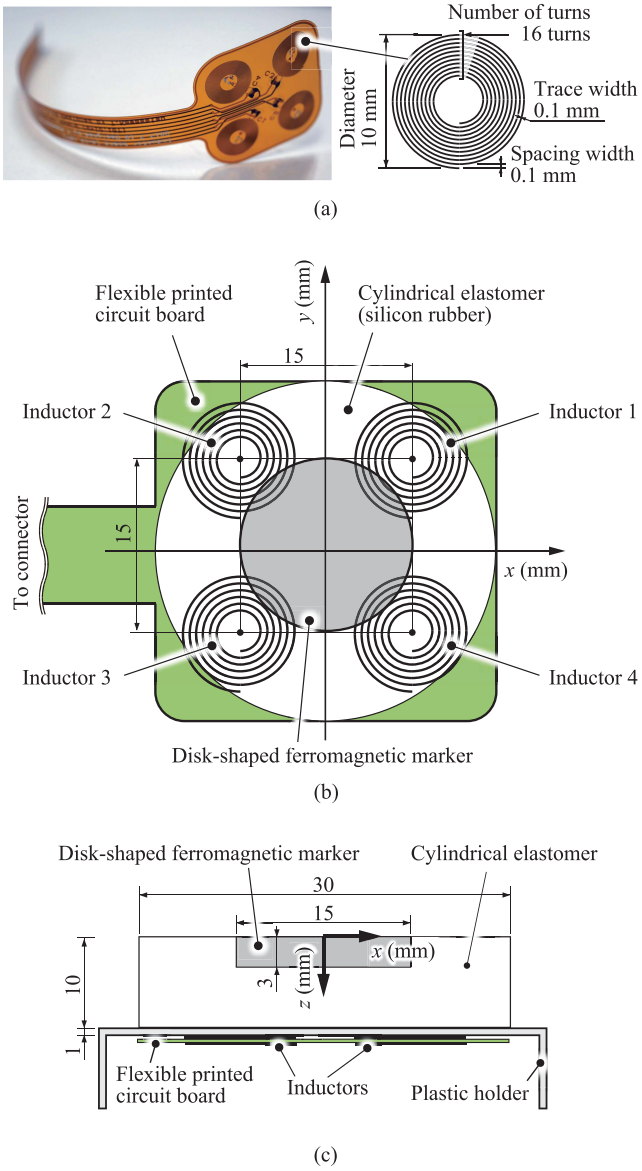

Fig. 3. Schematic and design parameters of the developed tri-axis tactile sensor: (a) design parameters for an inductor printed on the FPCB; (b) arrangement of inductors and ferromagnetic marker in x-y plane; and (c) arrangement of inductors and ferromagnetic marker in x-z plane.

B. Sensing Mechanism

The aggregation of iron particles are supported elastically on the inductors in the proposed sensor. Because the ferromagnetic marker containing iron particles function as a magnetic core for the inductors, the positional relationship between the marker and inductor determines its inductance (see also [4]). As shown in Figs. 1 and 3, the ferromagnetic marker is placed in the center of the four-inductor array where the marker is slightly raised from the array surface. Because the tri-axis force applied to the sensor surface causes a 3D displacement of the marker above the inductors, their inductances change in accordance with the distance between the marker and each inductor. In this structure, vertical displacements of the marker along the z-axis induced by the normal force F_z will increase the inductances of all the inductors. In contrast, horizontal

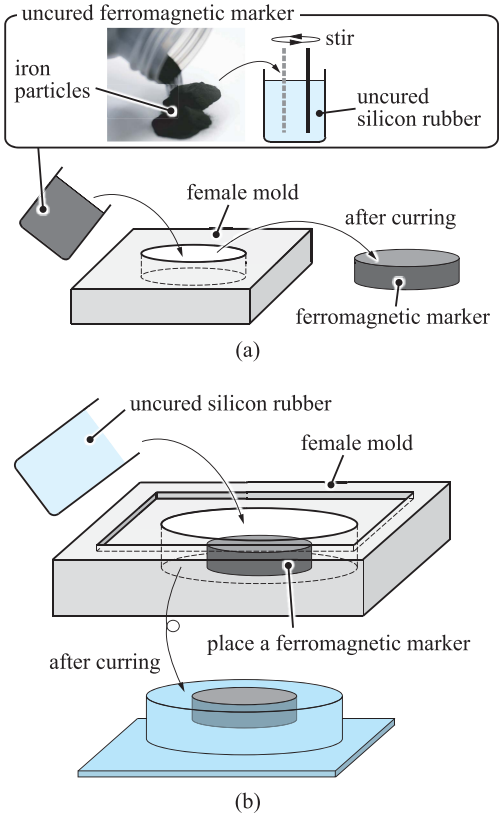

Fig. 4. Fabrication processes: (a) a ferromagnetic marker and (b) a cylindrical elastomer containing the ferromagnetic marker.

displacements of the marker along the x- or y-axes induced by shear forces F_x or F_y will increase/decrease the inductances of the inductors where the marker approaches/departs.

We assume that the applied force can be approximated by calculating the summation and difference of the four inductances as follows:

$$\begin{aligned} L_x &= (L_1 + L_4) - (L_2 + L_3) \\ L_y &= (L_1 + L_2) - (L_3 + L_4) \\ L_z &= L_1 + L_2 + L_3 + L_4 \end{aligned} \tag{1}$$

where L_i is the measured inductance of the i-th inductor. L_x and L_y are the differences in inductances along the x- or y-axes, while L_z is the summation of all inductances. The tri-axis forces F_x, F_y, and F_z are considered to be estimated from these converted inductances L_x, L_y, and L_z, respectively, by determining the relationship between these values.

IV. Experiments

The sensor response versus applied tri-axis force was measured with the experimental setup illustrated in Fig. 5. The developed sensor is attached to a tri-axis robot stage (TTA-C3-WA-30-25-10, IAI Corp., Japan) holding a force–torque sensor (F/T sensor; Mini 2/10-A, BL Autotech Ltd., Japan). As a contact target, a flat surface plastic indenter is attached to the tip of the F/T sensor. A personal computer (PC) captures the outputs of the F/T sensor via a 16-bit analog-to-digital converter (AI-1664LAX-USB,

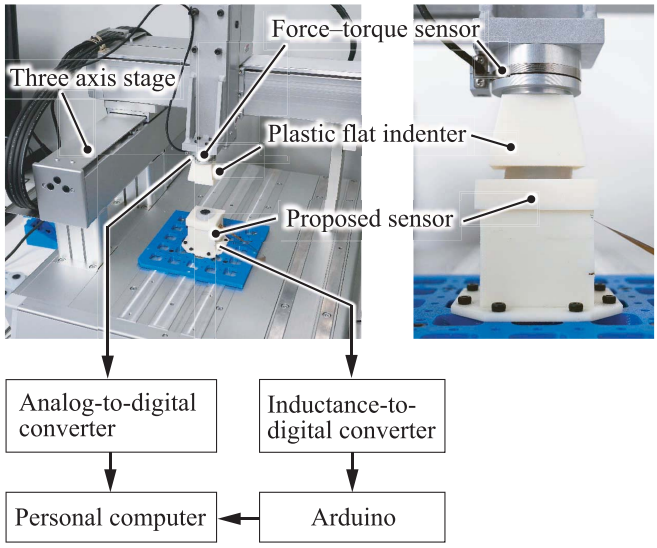

Fig. 5. Experimental setup for investigating the sensor responses. The proposed sensor is mounted on a three-axis robot stage holding a force–torque sensor (F/T sensor). Contact force is applied to the sensor using a plastic flat object attached to the tip of the F/T sensor. An inductance-to-digital converter measures the inductances and sends them to a personal computer (PC), while an analog-to-digital converter captures the output of the F/T sensor and sends it to the PC.

CONTEC Corp., Japan). A 28-bit inductance-to-digital converter (LDC1614EVM [24], Texas Instruments Corp., USA) captures the inductances of the sensor and sends their values to the PC via an Arduino board (Arduino Uno, Italy). In this experiment, the inductances of four inductors were measured one-by-one by switching the inductor activated with 200 μ A. The sampling period of both outputs of the F/T sensor and converted inductances was set to 20 ms.

Before the experiments, we measured the initial inductances of the four inductors, i.e., inductances under no load; the inductances were as follows: $L_1 = 8.2053$, $L_2 = 8.2588$, $L_3 = 8.1966$, and $L_4 = 8.2516$ μ H.

A. Sensor Calibrations

We investigated the sensor responses versus the applied tri-axis force to determine the relationships between the tri-axis force and the converted inductances calculated using Eq. 1. First, the normal force F_z was applied to the sensor by lowering the indenter at a speed of 0.1 mm/s until the surface of the sensor descended to a depth of 2.5 mm. Figure 6 shows the changes in the converted inductance L_z versus the applied normal force F_z. The measured shear forces F_x and F_y and converted inductances L_x and L_y are also depicted for reference because F_x and F_y were lightly applied to the sensor surface even when the application of F_z was intended. The solid line and shaded gray regions indicate the mean value and twice the standard deviation (2σ) of each inductance value across 10 trials, respectively. The dotted line indicates the mean value of the measured shear forces F_x and F_y across 10 trials. The result demonstrates that the value of L_z monotonically and linearly increases with the applied normal force F_z, while the values of L_x and L_y do not significantly

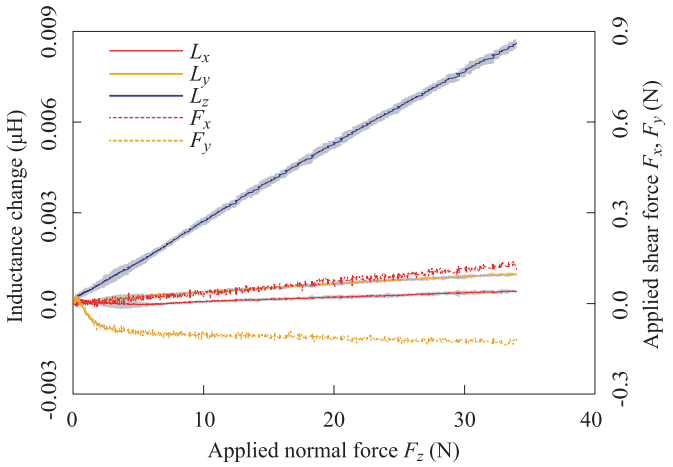

Fig. 6. Converted inductances L_x, L_y, and L_z versus the applied normal force F_z across 10 trials. The solid and dotted lines indicate the mean value of the converted inductance and applied shear force, respectively. The shaded region indicates twice the standard deviation (2σ) of each inductance. The inductance value L_z increases with the applied normal force, while L_x and L_y do not significantly increase.

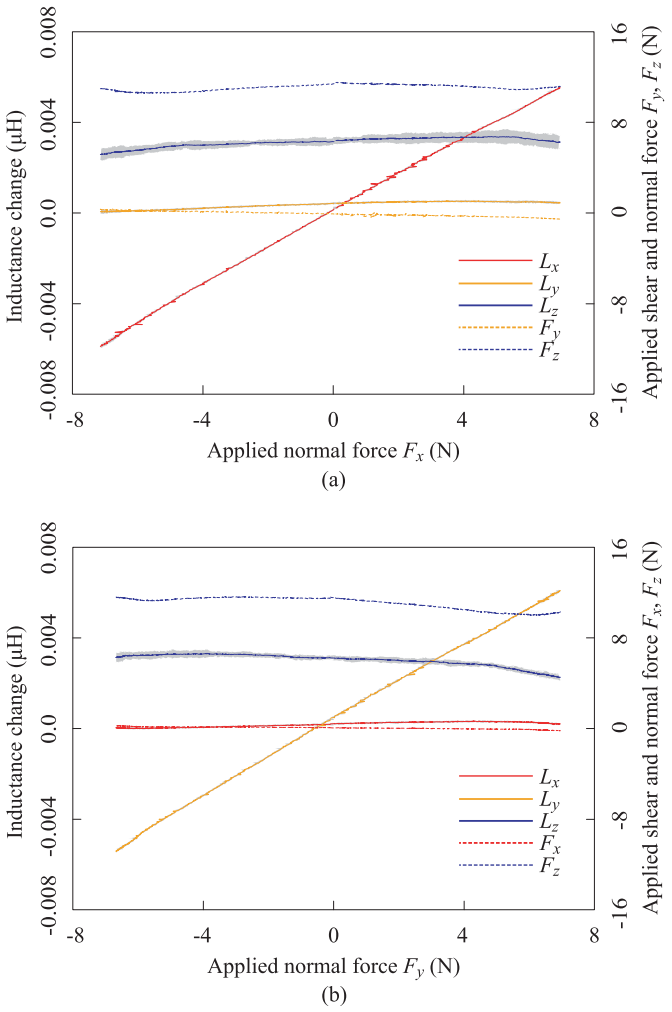

Fig. 7. Converted inductances versus the applied shear force (a) F_x and (b) F_y across 10 trials. The solid and dotted lines indicate the mean values of the converted inductance and applied shear and normal force, respectively. The shaded region indicates twice the standard deviation (2σ) of the inductance. Both plots demonstrate that the converted inductance value L_x and L_y increase in accordance with the applied shear force F_x and F_y, respectively, while L_z does not significantly increase.

increase with F_z. Therefore, the applied normal force F_z can be estimated by employing a linear function of L_z, i.e., the summation of the four inductances.

Next, the shear forces F_x and F_y were applied to the sensor with the following procedure: (1) apply a vertical deformation of 1 mm before applying a shear force; (2) horizontally move indenter ± 6 mm from the origin along x- or y-axes. Figure 7(a) shows the converted inductance L_x versus the applied shear force F_x, while (b) shows the converted inductance L_y versus the applied shear force F_y. In these plots, the other measured axis force and converted inductances are also depicted for reference. The solid line and shaded regions indicate the mean value and twice the standard deviation (2σ) of each inductance across 10 trials, respectively. The dotted line indicates the mean value of the other measured axis force across 10 trials. These results indicate that the values of L_x and L_y also monotonically and linearly increase with the applied shear force F_x and F_y. Therefore, the applied shear forces F_x and F_y can also be estimated by employing a linear function of L_x and L_y, i.e., the difference of the four inductances (Eq. 1).

From these results, the tri-axis force applied to the proposed sensor can be estimated based on the three converted inductance values of L_x, L_y, and L_z because these values monotonically, linearly, and almost independently increase in accordance with the applied shear forces F_x and F_y, and normal force F_z, respectively. Thus, the tri-axis force can be simply estimated from these inductance values as follows:

$$\begin{aligned} F_x &= a_x L_x + b_x \\ F_y &= a_y L_y + b_y \\ F_z &= a_z L_z + b_z \end{aligned} \tag{2}$$

where a_i and b_i are constant values. A least-squares method was applied to obtain these constant values; these values were estimated as follows by using the results presented in Figs. 6 and 7: $a_x = 1.239 \times 10^3$, $b_x = -0.05104$, $a_y = 1.192 \times 10^3$, $b_y = -0.4377$, $a_z = 3.889 \times 10^3$, and $b_z = -0.4855$. In addition, the fitting errors R were $R_x = 0.9961$, $R_y = 0.9900$, $R_z = 0.9989$.

To evaluate the measurement noise, we calculated the maximum variance of L_x, L_y, and L_z when applying F_x, F_y, and F_z, respectively; these values were 3.445×10^{-9}, 1.237×10^{-8}, and 1.427×10^{-8} μH^2 for L_x, L_y, and L_z, respectively. From Fig. 7, the small 2σ regions of L_x and L_y compared to their range of inductance change demonstrate a high repeatability of those inductances across 10 trials. In contrast, the 2σ region of L_z shown in Fig. 6 is larger compared with that of L_x and L_y. In addition, the signal-to-noise ratio (SNR) was evaluated using the following equation: $20\log10(A_S/A_N)$ where A_S is the maximum peak-to-peak inductance change from the initial inductance and A_N is the maximum peak-to-peak inductance change under no load. The SNRs of L_x, L_y, and L_z were 40.77, 42.53, and 34.19 dB, respectively. To evaluate the sensitivity of the sensor, we calculated the minimum detectable

TABLE I
ROOT MEAN SQUARED ERRORS BETWEEN THE ESTIMATED AND MEASURED TRI-AXIS FORCE ACROSS 10 TRIALS

	F_x	F_y	F_z
average (N)	0.455	0.704	1.21
variance (N^2)	0.761×10^2	0.435×10^2	9.49×10^2

force S for three orthogonal directions; these values can be calculated using the results in Figs. 6 and 7, as well as the obtained noise levels: $S_x = 94.4$ mN, $S_y = 173$ mN, and $S_z = 444$ mN.

B. Tri-Axis Force Sensing

We next evaluated the estimated tri-axis force based on the obtained relationship between the applied force and inductance change, as described in Section IV-A. The tri-axis forces were simultaneously applied to the sensor with the following procedure: (1) apply a vertical deformation of 0.5 mm with a contact speed of 20 mm/s; (2) horizontally move indenter to the position $(x, y) = (3, -3)$ with a contact speed of 1 mm/s; (3) move indenter to the position $(x, y) = (-3, 3)$ with a contact speed of 20 mm/s; (4) apply additional 0.5-mm vertical deformation with a contact speed of 20 mm/s. Then, repeat 2) to 4) until the applied vertical deformation reaches 2 mm.

Figure 8 represents the relationship between the estimated force and applied tri-axis force versus time. The solid gray line indicates the applied tri-axis force F measured with the F/T sensor, while the solid black line indicates the estimated tri-axis force F_{est} based on the measured inductances. In addition, the dotted red line represents the estimation error, i.e. $F - F_{est}$, for reference. The result demonstrates a good agreement between the estimated tri-axis force and the applied tri-axis force. However, the estimation error increases under a large applied normal force. In addition, the estimation error is large during the fast contact condition, i.e., during the procedure of (3) described above. To evaluate the estimation error, we calculated the root mean squared errors (RMSE) between the estimated and measured tri-axis forces. We measured the tri-axis force 10 times with the same procedure described above, and obtained the average and variance of the RMSEs, as summarized in table I.

V. DISCUSSIONS

This section first summarizes the sensor response curves describing the relationship between the inductance changes and the applied tri-axis force. Then, we discuss the estimation results of the applied tri-axis force based on the assumed linear function. Finally, we summarize the advantages of the proposed sensor.

A. Sensor Calibration and Tri-Axis Force Sensing

The experimental results indicate that the proposed tri-axis tactile sensor can measure the three-axis force by monitoring the changes in the inductances from the four inductors. In this study, we define three converted inductance values L_x, L_y, and L_z as the simple summation or difference of the four inductances (Eq. 1), and we found that the relationship between these values and the applied tri-axis force can be given with a simple linear function (Eq. 2), although the sensor consists of a highly soft rubber.

The result in Section IV-B demonstrates that the sensor can estimate the tri-axis force based on the inductance values by using the obtained linear functions described in Eq. 2. We found that the estimation errors increased with the applied normal force. One potential reason for this estimation error could be the deformation of the ferromagnetic marker itself. The marker could deform when a large contact force was applied because the marker itself is composed of a highly soft and flexible silicon rubber. This deformation of the marker will become large under a large applied contact force and cause the estimation error. Therefore, the proposed sensor works well under a contact force that causes little to no deformations of the marker. In this study, the ferromagnetic marker deformed because we employed the same soft silicon rubber with the cylindrical elastomer to construct the ferromagnetic marker. Employing a ferromagnetic marker composed of a hard-type rubber could reduce the deformation of the marker; however, employing such a hard-type rubber deteriorates the softness of the surface rubber. Therefore, one of the issues is that the deformation of the ferromagnetic marker should be reduced without employing the hard-type rubber.

The result also indicates that the estimation error was large during the fast contact condition, e.g., the force curves at about 5, 15, and 25 s in Fig. 8. We also found that the estimated force had a time-delay compared to the measured force during the fast contact condition. This time-delay appears to be caused by the viscosity of the employed rubbers because the deformation of the rubbers requires a few transient times because of its viscosity. Therefore, the output of the proposed sensor has a short time delay to the actual applied force. One of the solutions to this issue is the use of another low-viscosity elastic material instead of the silicon rubber holding the ferromagnetic marker, e.g., a soft sponge, as we employed in [25].

B. Advantages of the Proposed Sensor

The structure of the proposed sensor is quite simple: an elastic material holding a rubber with iron particles is simply placed on four spiral inductors. In the proposed sensing mechanism, a trace on an FPCB itself, i.e., an inductor, becomes a tactile transducer. The proposed sensor can be mounted on a complicated surface because the sensor only consists of a soft and stretchable surface rubber and a bendable FPCB. In this study, we employed a printed circular spiral inductor as the sensing inductor for the following reasons: first, printed circular spiral inductors enable us to fabricate thin FPCB easier compared to other inductors, e.g. rectangular, triangular spiral coils or wound up coils; second, the spatial response properties of printed circular spiral inductors have been investigated in [4]. Although the sensing mechanism allows us to employ other inductor shapes, the sensitivity and accuracy of tri-axis force measurements would depend on the inductors type. One of the future issues is to investigate how inductor shape affects its sensor response.

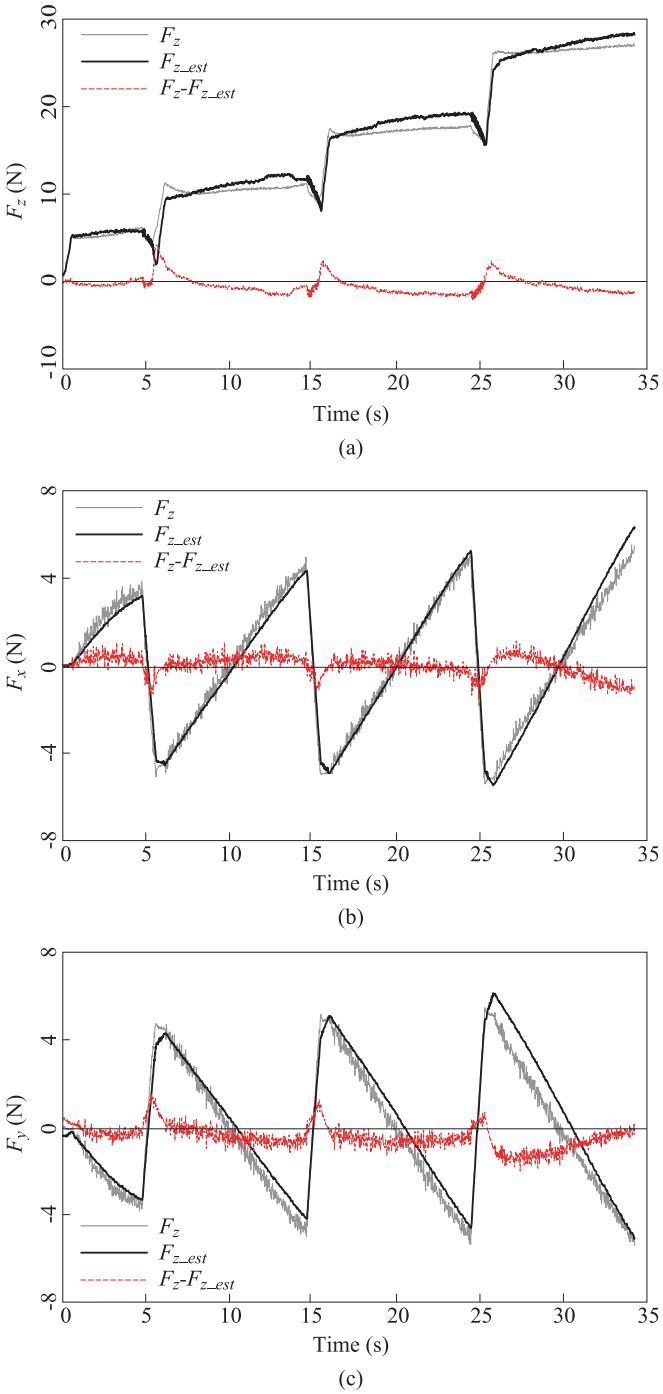

Fig. 8. Comparison between measured and estimated tri-axis force applied to the proposed sensor: (a) applied normal force F_z versus time; (b), (c) applied shear force F_x and F_y versus time, respectively. The solid gray line indicates the measured tri-axis force with the F/T sensor (i.e., reference force), while the solid black line indicates the estimated tri-axis force based on the measured inductance values. The dotted red line indicates the estimation error, i.e., difference of the measured and estimated force, for reference.

The greatest advantage of the sensor is that the sensor surface is composed of only a soft and stretchable rubber, and this surface rubber can be placed to the outside of the frame containing its measurement circuit inside (as we placed the rubber on the plastic holder holding the FPCB). This separation between the rubber and the FPCB with the corresponding measurement circuits leads to a number of advantages: 1) the fragile elements such as the printed circuits and ceramic capacitors are protected from the contact force to reach. Thus, the proposed sensor has high durability against large contact forces; 2) it is easy to replace its surface when the surface is damaged; 3) the sensor can be used in water, which has an equivalent magnetic permeability as air, because the sensor structure can be waterproof by placing the sensing elements inside a waterproof holder. We are certain these advantages will facilitate a number of applications of the proposed sensor.

VI. Conclusion

In this article, we proposed a flexible tri-axis tactile sensor using four spiral inductors and a ferromagnetic marker embedded in a cylindrical elastomer made of a silicon rubber. In this study, we measured the sensor responses using the developed sensor in order to investigate the relationship between the applied tri-axis force and inductance changes. The experiments demonstrated that the proposed sensor can simply estimate the applied tri-axis force based on simple linear functions of three converted inductance values, i.e., the summation and difference of four inductances. In contrast, we also found that a large applied force can cause a large estimation error because the soft ferromagnetic marker itself can be deformed with respect to the applied force.

In this study, we mounted an FPCB and rubbers on a flat plastic holder. As one of future works, the proposed sensor could be mounted to an arbitrary surface shape on a complex-shaped surface, e.g., a curved surface, and the effect to its response property upon deformation of the FPCB and rubbers could be investigated. An additional step is to mount the proposed sensor on the tip of a robot hand or body of a robot for further testing. We are certain that the simple-structured proposed sensor of high durability will accelerate the utilization of tactile sensors in robots. One of the issues for future discussions is the extent to which external magnetic sources such as electric motors and movable metallic parts of the robot itself can deteriorate the sensor performance.

The advantage of our sensor for miniaturization is that only the printed inductor circuits and ferromagnetic particles are required in the sensing areas. This simple structure potentially enables us to fabricate a sensor with a smaller taxel size and thinner thickness than the ones fabricated in this study. This miniaturization is one of our future issues.

Acknowledgment

The authors would like to thank Mr. Hiroaki Ota for his valuable advice on the sensing mechanism.

References

[1] R. S. Dahiya, G. Metta, M. Valle, and G. Sandini, "Tactile sensing—From humans to humanoids," *IEEE Trans. Robot.*, vol. 26, no. 1, pp. 1–20, Feb. 2010.
[2] H. Yousef, M. Boukallel, and K. Althoefer, "Tactile sensing for dexterous in-hand manipulation in robotics—A review," *Sens. Actuators A, Phys.*, vol. 167, no. 2, pp. 171–187, 2011.
[3] B. D. Argall and A. G. Billard, "A survey of tactile human–robot interactions," *Robot. Auton. Syst.*, vol. 58, no. 10, pp. 1159–1176, 2010.

[4] T. Kawasetsu, T. Horii, H. Ishihara, and M. Asada, "Size dependency in sensor response of a flexible tactile sensor based on inductance measurement," in *Proc. IEEE Sens. Conf.*, Oct. 2017, pp. 1–3.
[5] N. Thanh-Vinh, N. Binh-Khiemb, H. Takahashi, K. Matsumoto, and I. Shimoyama, "High-sensitivity triaxial tactile sensor with elastic microstructures pressing on piezoresistive cantilevers," *Sens. Actuators A, Phys.*, vol. 215, pp. 167–175, Aug. 2014.
[6] H. Takahashi, A. Nakai, N. Thanh-Vinh, K. Matsumoto, and I. Shimoyama, "A triaxial tactile sensor without crosstalk using pairs of piezoresistive beams with sidewall doping," *Sens. Actuators A, Phys.*, vol. 199, pp. 43–48, Sep. 2013.
[7] K. Hosoda, Y. Tada, and M. Asada, "Anthropomorphic robotic soft fingertip with randomly distributed receptors," *Robot. Auto. Syst.*, vol. 54, no. 2, pp. 104–109, 2006.
[8] D. Hirashima, T. Uematsu, M. Sohgawa, W. Mito, and T. Kanashima, "Fabrication of a flexible array for tactile sensors with microcantilevers and the measurement of the distribution of normal and shear forces," *Jpn. J. Appl. Phys.*, vol. 50, no. 6S, p. 06GM02, 2011.
[9] Y.-M. Huang, N.-C. Tsai, and J.-Y. Lai, "Development of tactile sensors for simultaneous, detection of normal and shear stresses," *Sens. Actuators A, Phys.*, vol. 159, no. 2, pp. 189–195, 2010.
[10] S. Zhao, Y. Li, and C. Liu, "A tri-axial touch sensor with direct silicon to PC-board packaging," *Sens. Actuators A, Phys.*, vol. 170, nos. 1–2, pp. 90–99, 2011.
[11] T. P. Tomo *et al.*, "Design and characterization of a three-axis Hall effect-based soft skin sensor," *MDPI Sens.*, vol. 16, no. 4, p. 491, 2016.
[12] S. Youssefian, N. Rahbar, and E. Torres-Jara, "Contact behavior of soft spherical tactile sensors," *IEEE Sensors J.*, vol. 14, no. 5, pp. 1435–1442, May 2014.
[13] L. Jamone, L. Natale, G. Metta, and G. Sandini, "Highly sensitive soft tactile sensors for an anthropomorphic robotic hand," *IEEE Sensors J.*, vol. 15, no. 8, pp. 4226–4233, Aug. 2015.
[14] M. Goka, H. Nakamoto, and S. Takenawa, "A magnetic type tactile sensor by GMR elements and inductors," in *Proc. IEEE/RSJ Int. Conf. Intell. Robots Syst. (IROS)*, Oct. 2010, pp. 885–890.
[15] Y. Liu, H. Han, T. Liu, J. Yi, Q. Li, and Y. Inoue, "A novel tactile sensor with electromagnetic induction and its application on stick-slip interaction detection," *Sensors*, vol. 16, no. 4, pp. 430–445, 2016.
[16] T. P. Tomo *et al.*, "Covering a robot fingertip with uSkin: A soft electronic skin with distributed 3-axis force sensitive elements for robot hands," *IEEE Robot. Autom. Lett.*, vol. 3, no. 1, pp. 124–131, Jan. 2018.
[17] A. Takagi, Y. Yamamoto, M. Ohka, H. Yussof, and S. C. Abdullah, "Sensitivity-enhancing all-in-type optical three-axis tactile sensor mounted on articulated robotic fingers," *Procedia Comput. Sci.*, vol. 76, pp. 95–100, Jan. 2015.
[18] K. Kamiyama, K. Vlack, T. Mizota, H. Kajimoto, K. Kawakami, and S. Tachi, "Vision-based sensor for real-time measuring of surface traction fields," *IEEE Comput. Graph. Appl.*, vol. 25, no. 1, pp. 68–75, Jan. 2005.
[19] A. Yamaguchi and C. G. Atkeson, "Combining finger vision and optical tactile sensing: reducing and handling errors while cutting vegetables," in *Proc. IEEE-RAS 16th Int. Conf. Humanoid Robots (Humanoids)*, Nov. 2016, pp. 1045–1051.
[20] K. Kamiyama, H. Kajimoto, N. Kawakami, and S. Tachi, "Evaluation of a vision-based tactile sensor," in *Proc. IEEE Int. Conf. Robot. Autom. (ICRA)*, Apr. 2004, pp. 1542–1547.
[21] Y. Ito, Y. Kim, and G. Obinata, "Robust slippage degree estimation based on reference update of vision-based tactile sensor," *IEEE Sensors J.*, vol. 11, no. 9, pp. 2037–2047, Sep. 2011.
[22] L. Cramphorn, B. Ward-Cherrier, and N. F. Lepora, "Tactile manipulation with biomimetic active touch," in *Proc. IEEE Int. Conf. Robot. Autom. (ICRA)*, May 2016, pp. 123–129.
[23] H. Wang, J. Kow, G. de Boer, D. Jones, A. Alazmani, and P. Culmer, "A low-cost, high-performance, soft tri-axis tactile sensor based on eddy-current effect," in *Proc. IEEE Sens. Conf.*, Oct./Nov. 2017, pp. 666–668.
[24] Texas Instruments. *Inductance-to-Digital Converter Chip LDC1614*. Accessed: May 30, 2018. [Online]. Available: http://www.ti.com/product/LDC1614/
[25] T. Kawasetsu, T. Horii, H. Ishihara, and M. Asada, "Mexican-hat-like response in a flexible tactile sensor using a magnetorheological elastomer," *Sensors*, vol. 18, no. 2, p. 587, 2018.

Takumi Kawasetsu is currently pursuing the Ph.D. degree with the Department of Adaptive Machine Systems, Graduate School of Engineering, Osaka University, Osaka, Japan. He is a Research Fellow of the Japan Society for the Promotion of Science. His research interests include tactile sensors, tactile information processing, visual information processing in biological systems, and spiking neural networks.

Takato Horii received the M.E. degree from the Department of Adaptive Machine Systems, Graduate School of Engineering, Osaka University, Osaka, Japan, in 2012. He is currently a Project Assistant Professor with the Graduate School of Informatics and Engineering, University of Electro-Communications. He was a Research Fellow of the Japan Society for the Promotion of Science. His research interests include the computational modeling of emotion, emotional human–robot communication, and tactile interaction. He was a Research Fellow of the Japan Society for the Promotion of Science.

Hisashi Ishihara received the Ph.D. degree from the Department of Adaptive Machine Systems, Graduate School of Engineering, Osaka University, Osaka, Japan, in 2012. He is currently a Tenured Track Assistant Professor with the Graduate School of Engineering, Osaka University. He is also a PRESTO Researcher with the Japan Science and Technology Agency, a Visiting Researcher with the RIKEN Brain Science Institute, and a Collaborating Researcher with ATR. His research interests include android engineering for developing human-friendly android robots.

Minoru Asada received the B.E., M.E., and Ph.D. degrees in control engineering from Osaka University, Osaka, Japan, in 1977, 1979, and 1982, respectively. In 1995, he joined Osaka University as a Professor, where he has been a Professor with the Department of Adaptive Machine Systems, Graduate School of Engineering, since 1997. Dr. Asada received many awards such as the Best Paper Award at the IEEE/RSJ International Conference on Intelligent Robots and Systems (IROS92) and a Commendation by the Minister of Education, Culture, Sports, Science and Technology, Japanese Government, as a Person of Distinguished Services to Enlightening People on Science and Technology. He is one of the founders of the RoboCup and former President of the International RoboCup Federation (2002–2008). He was the Research Director of the ASADA Synergistic Intelligence Project at Exploratory Research for Advanced Technology by the Japan Science and Technology Agency (ERATO, 2005–2011) and a Principal Investigator of the Grants-in-Aid for Scientific Research (Research Project Number: 24000012) from 2012 to 2016. He is currently a Principal Investigator of the JST RISTEX Research and Development Project titled Legal Beings: Electric personhoods of artificial intelligence and robots in NAJIMI Society, based on a reconsideration of the concept of autonomy.